Resilient New Space Communication using Cognitive Radio for LEO Satellites

Rathinamala Vijay*, Jens Freymuth†, Alexander Burnicki†, Enrico Stoll†, Falko Dressler*
* School of Electrical Engineering and Computer Science, TU Berlin, Germany
† Chair of Space Technology, TU Berlin, Germany
{rathinamala.vijay, jens.freymuth, alexander.burnicki, e.stoll, dressler}@tu-berlin.de

***Abstract*—Non-terrestrial networking is one of the core technologies for next generation communication networks due to the achievable coverage and resilience. The number of LEO satellites in orbit have increased due to cost reduction in cubesat development and launch services. This grow in users can lead to higher noise levels and increase interference among satellite and terrestrial networks. Innovative space communications using software defined radio (SDR) technology can solve the contention between the LEO satellites and enables them to coexist with terrestrial network. In this paper, we investigate the use of cognitive radio concepts for LEO satellites. In particular, we focus on interference detection and appropriate channel switching. The key objective is to provide resilient communication for critical infrastructure. Using both results from an already launched cubesat system as well as from a testbed experiment, we demonstrate the feasibility of our approach.**

***Index Terms*—New space communication, interference detection, cognitive radio, software defined radio.**

I. Introduction

There are cases of emergency situation where the ground infrastructure is damaged due to natural disasters such as earthquakes, avalanches, and tsunamis. In these situations, setting up a communication network within a short time is essential. LEO satellites are considered to fill this gap, to receive messages from inter-satellite communication and relay the obtained message to the mobile receiver at the ground [1], [2]. In general, new space communication (NeSC) systems enable a symbiotic relation between satellite and terrestrial communications. The increasing number of low earth orbit (LEO) satellite constellations support the realization of resilient networks that can provide redundant channels to the terrestrial networks and mitigates jamming and interference effects. Further, in 6G communications, the satellite and terrestrial networks will coexist to increase the global coverage [3]. This motivates the satellite operators to use cognitive radio in high-altitude platform station (HAPS) as well as LEO and medium earth orbit (MEO) satellite communication systems. For example, the offshore wind turbines are becoming ever more important for our energy infrastructure. Acquiring data from remote areas is challenging and there is a clear need for designing communication networks to monitor critical infrastructures reliably amidst interference scenarios. For this relaying from these offshore locations, a number of challenges needs to be addressed. This includes frequency allocation (including channel selection), interference mitigation (concerning other satellite links as well as noise spikes due to solar flares), power consumption, and time synchronization [1], [4].

Software defined radios (SDRs) are widely used in today's cubesats as physical layer parameters and even the waveform can be changed dynamically in NeSC systems [5], [6]. This particularly also holds to improve physical layer resilience [7]. Also, SDRs provide the basic functionality for accurate sensing of the environment [8]. Our approach to mitigate the interference is developing a SDR-based cognitive radio system at both the satellite and terrestrial nodes that communicate with each other. The cognitive radio will perform spectrum sensing and spectrum allocation techniques for efficient wireless resource management [9]–[11]. In particular, we evaluate two spectrum sensing techniques namely energy detection (ED) and absolute value cumulating (AVC) [12].

In-orbit spectrum sensing and interference measurement are carried out by very few missions [6], [13], [14]. Recently, the publicly available database of global interference measurement from the Spectrum AnaLysis SATellite (SALSAT) was released.[1] SALSAT is a nano satellite launched by the chair of space technology at TU Berlin in September 2020. The satellite is operating in a sun-synchronous orbit around Earth. The mission features a SDR based payload SALSA with a LMS7002 transceiver and analyzes amateur radio bands VHF, UHF as well as S-band for investigation of spectrum usage. The interference analysis of captured spectrum data in SALSAT can be partially performed by a Linux-based processing system. However, the analysis is mostly performed on ground [14]. In the follow-up project Robust And seCure post quantum COmmunication fOr critical iNfrastructure (RACCOON)[2] [15], the on-board SDR will perform interference analysis and take corrective actions if needed.

The research question we answer in this paper is how to realize a satellite connection that is resilient to interference and unexpected noise conditions. We present a spectrum sensing approach and discuss some initial results from both a lab experiment as well as an experiment using the SALSAT data.

Our main contributions can be summarized as follows:

- We present a cognitive radio-based algorithm for channel allocation based on interference class assessment for each subchannel in a band.

[1] https://salsat.raumfahrttechnik.tu-berlin.de/

[2] https://www.tu.berlin/en/raumfahrttechnik/research/current-projects/raccoon/

- We present a backup channel prediction method based on the data collected from the SDR transceiver located in SALSAT satellite launched by TU Berlin that is in orbit since 2020.
- We developed an SDR testbed to demonstrate the interference classification based on Kolmogrov-Smirnov test.

II. Related Work

Cognitive radio allows to adapt parameters, such as frequency, antenna, and time of transmission based on the current situation on the radio channels. Cognitive radio techniques are considered very mature in the literature, despite the limited deployment in commercial applications [16]–[18]. In the domain of satellite communication, cognitive radio faces new challenges related to spectrum sensing in the presence of non-Gaussian noise and insufficient time-synchronization between ground station and satellites [19]. Here, correct interference analysis is crucial to find a solution to these challenges. Uplink radio interference in UHF band is considered by Quintana-Diaz et al. [13]. The authors study dispersion and time variation of the interference using an SDR on-board the LUME-I satellite. They conclude that communication systems that are designed for additive white Gaussian noise (AWGN) channels are not able to communicate with their satellites in the presence of space-tracking radars that causes high coefficient of variation [13].

Spectrum sensing techniques that do not need prior knowledge of the primary signal and channel model are easier to implement [12], [20], [21]. These low complexity implementations translate to low power consumption on-board a satellite. Simple concepts like ED do not work appropriately as their performance decreases with low signal to interference and noise ratio (SINR) scenarios and noise variance uncertainty [22], [23]. Instead, we use the Kolmogrov-Smirnov (KS) based goodness of fit test that is combination with ED for interference classification.

As an alternative, Aghabeiki et al. [24] present a machine learning (ML)-based spectrum sensing algorithm to improve the primary signal detection under low SINR conditions. The ML algorithm allows to learn signal properties and propagation channel features. In addition, the authors use principal component analysis to extract the uncorrelated data. In our proposed work, ML algorithms are used to model the joint distribution of probability of detection and probability of false alarms from energy detection. Furthermore, we apply the "Kolmogrov-Smirnov one class over rest of the class", KS_{OvR} test to classify three interference classes.

III. System Model

Figure 1 shows the orbital plane of a satellite S1 and the reference plane. Satellite S2 is the interference source at the receiver. The orbit of the satellite is represented by parameters such as the semi-major axis of the orbit r, the inclination angle of the satellite orbit with respect to the reference plane, i, and the longitude angle, θ. The inclination angle, i of the satellite orbit is 95 degree. The semi-major axis of the satellite orbit, r is

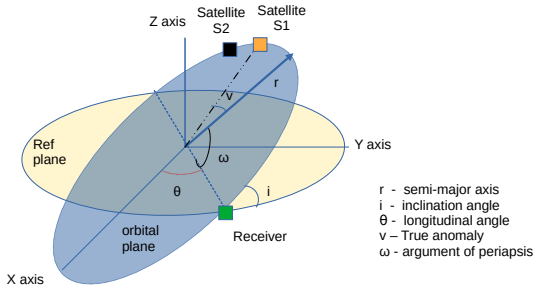

Figure 1. The orbital plane and reference planes of the LEO satellites S1 and S2 are defined by Keplerian elements shown in figure. The reference plane considered is ECEF coordinate system.

575 km at the time of deployment. The primary purpose of this satellite is collecting RF spectrum data over frequencies that are often used in small satellite communications [6]. The coverage probability for the LEO satellite with dynamic interference scenario is calculated as [25], [26]

$$P(SINR > \lambda) = P\left(\frac{p_{tx} H g_a ||(X-l)||^{-\alpha}}{\sigma^2 + I_l} > \lambda\right) \quad (1)$$

where λ is the SINR threshold beyond which the satellite coverage is stable. p_{tx} is the transmit power of the LEO satellite. H is the fading random variable modelled using Nagakami-m small-scale fading that includes both the Line of Sight (LOS) and the Non-Line of Sight (NLOS) scenarios and proved to be an appropriate channel model for the satellite to ground links. Nagakami-m distribution assumes that the LOS component obeys the gamma distribution. When $m = 1$, then the Nagakami reduces to Rayleigh fading and when $m = \frac{(K+1)^2}{2K+1}$ where K is the Ricean factor that quantifies the ratio of power of the direct signal and that of the scattered paths. The probability density function (PDF) for H is given by [25]

$$f_H(x) = \frac{2m^m}{W^m(m-1)!} x^{2m-1} \exp\left(\frac{-mx^2}{W}\right) \quad (2)$$

where W is the average power of the envelope, g_a is the transmit antenna gain, X is the position of the LEO satellite, l is the position of the receiver, σ^2 is the noise variance, and I_l is the interference seen by the receiver located at l due to other LEO and GEO satellites, HAPS, or terrestrial networks and is given by [25]

$$I_l = \sum_{i=1}^{n} p_{tx_i} H_i g_{a_i} ||X_i - l||^{-\alpha_i} \quad (3)$$

where p_{tx_i} is the transmit power of i^{th} interference source located at position, and H_i, α_i, g_{a_i} are the fading random variable, path loss exponent, and transmit antenna gain of the i^{th} interference source, respectively.

IV. Interference Analysis

Interference analysis helps in solving the spectrum contention among the satellite and terrestrial networks. As a first step

towards interference analysis, we classify the interference scenarios in each channel into three classes namely *Least*, *Medium*, and *Worst* interference scenarios. This classification aids in the assessment of the quality of the channel. Eventually this plays a major factor in spectrum allocation.

We propose Algorithm 1 for the classification of interference scenarios. γ_L, γ_M, and γ_W indicate the SINR at the least, medium, and worst interference scenarios. For this, the collective distribution of the probability of detection, P_d and probability of false alarm, P_{fa} corresponding to every γ measured at the receiver is considered. We then perform the multi-class Kolmogrov-Smirnov test to differentiate One class Over the Rest (OvR) of the classes. Here, $KS_{OvR}(n_W)$, $KS_{OvR}(n_M)$, and $KS_{OvR}(n_L)$ are the KS distance value of the least, medium, and worst interference case for the n^{th} channel compared to other two classes, respectively. cch_n and bch_n are the current and backup channels for the n^{th} channel. The main motivation to use KS test-based classification on receiver operating characteristics (ROC) metrics is that the test is effective even with small dataset [27].

Algorithm Walk-through: Algorithm has interference assessment phase and channel assignment phase. The interference assessment phase collects the spectrum sensing performance metrics for each channel for three SINR values. After collecting this data, split this data into training and test data. We perform random forest and naive Bayes classifier to fit the data for each class. Then KS_{OVR} test is performed for each class over rest of the class for the training data split and compute the thresholds for every class.

Next, in the channel assignment phase, the $KS_{OVR}(n_W)$, $KS_{OVR}(n_M)$, $KS_{OVR}(n_L)$ are evaluated for the instantaneous unclassified tuple (P_d^n, P_{fa}^n) values from the test data collection. Later we compare the values with thresholds to make a channel usage decision for n^{th} channel to stay idle, transmit in current channel cch_n, or move to a backup channel bch_n. The spectrum sensing and acquiring performance metrics from the SDR based testbed is described in the next section.

V. Testbed-based Evaluation

For evaluation and to obtain further insights of the system performance, we developed a SDR-based testbed as shown in Figure 2 to evaluate the spectrum sensing module. The testbed configurations are as detailed in Table I.

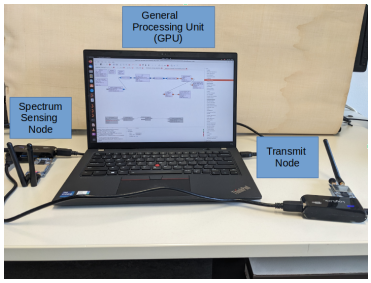

Figure 2. Spectrum sensing testbed to demonstrate interference classification

Algorithm 1: Interference assessment and channel selection algorithm

Data: $ch = \{1, 2, ..., N\}$ `// List of channels`
Data: S=$\{\gamma_W, \gamma_M, \gamma_L\}$ `// SINR for three interference classes`
`/* Interference Assessment Phase */`
foreach $n \in ch$ **do**
  foreach $\gamma \in S$ **do**
    $P_d^{n,\gamma} = P((T^n > \lambda)|H1)$
    $P_{fa}^{n,\gamma} = P((T^n > \lambda)|H0)$
    Apply classifier model to fit the data
    Perform KS_{OvR} test
    Compute thresholds th_w, th_m, th_l based on KS_{OvR} test
  end
end
`/*` KS_{OvR}`- KS test class over the rest of the class */`
`/* Channel Assignment Phase */`
foreach $n \in ch$ **do**
  if $KS_{OvR}(n_l) \geq th_l$ **then**
    $TXCH = cch_n$ `// current channel`
  else
    if $th_m \geq (KS_{OvR}(n_M)) \leq th_l$ **then**
      $TXCH = null$ `// idle`
    else
      $TXCH = bch_n$ `// backup channel`
    end
  end
end

A. GNU Radio Framework for Spectrum Sensing

Figure 3 shows the implementation of two spectrum sensing techniques in GNU Radio.[3] We have used this software framework to implement the following functionalities: (a) generating a LEO satellite transmit signal with 600 KHz

[3]https://www.gnuradio.org/

Table I
Spectrum sensing testbed configurations

Parameter	Value
Center Frequency	863 MHz
Sensing bandwidth	10 MHz
Channel bandwidth	600 KHz
Maximum Transmit power	20 dBm
Spectrum sensing node	LimeSDR mini v2
Interference nodes	USRP B205 mini, LimeSDR mini v2
Software	Ubuntu 22.04 GNU Radio 3.10.8.0

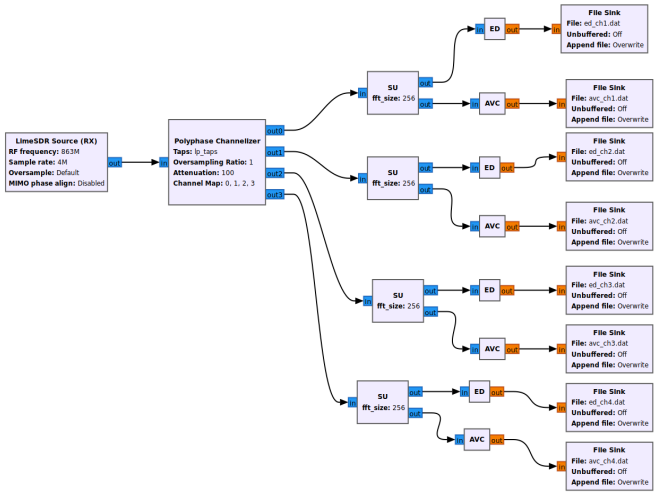

Figure 3. The ED and AVC spectrum sensing techniques to detect the interference as seen by a LEO satellite.

bandwidth, (b) generating interference source with multiple 600 KHz bandwidth signals; the probability of occurrence of interference sources P_{I_i} is derived from uniform distribution at every iteration, (c) implementing two spectrum sensing techniques namely ED and AVC [12], (d) computing probability of detection P_d and probability of false alarm P_{fa}.

In our testbed, we have the option to incorporate various channel losses such as antenna misalignment loss, polarization loss, RF cable loss, atmospheric loss due to weather conditions, multipath fading, and impact of Doppler effect. The receive chain in onboard SDR performs spectrum sensing. At every receive cycle a 10 MHz bandwidth channel is subdivided into four channels. The ED and AVC spectrum sensing techniques are semi-blind detection techniques where the knowledge of noise variance and its standard deviation is used. Our testbed is used to study the effect of each technique and the quality of interference analysis in the desired spectrum.

B. Experiments

For the experiment, the interference node is switched on and off with various transmit power levels. Based on the transmit power level, the SINR value changes at the receiver. At each transmit power level of the interference node, spectrum sensing is performed for 1000 iterations. The sensing bandwidth considered is 10 MHz and is subdivided into N channels. The test statistic value T^n of the n^{th} channel for ED is given by

$$T^n = (1/L) \sum_{i=1}^{L} |x(k)|^2 \tag{4}$$

The hypothesis $H0$ and $H1$ are described as

$$H0 : w(k) \tag{5}$$

$$H1 : x(k) + w(k) \tag{6}$$

where $w(k)$ is the noise sample and $x(k)$ is the interference signal samples of the n^{th} channel. The noise and signal samples are obtained using an SDR and signal acquisition blocks in the GNU Radio framework.

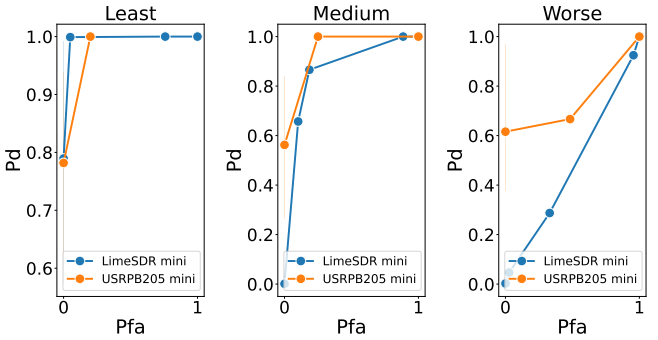

Figure 4. Receiver operating characteristics of spectrum sensing module under three interference scenarios.

- Step1: Compute the $P_d^{n,\gamma}$, probability of detection for n^{th} channel under SINR value γ by evaluating the probability of the test statistic of the n^{th} channel greater than the threshold λ given the hypothesis H1.
- Step2: Compute $P_{fa}^{n,\gamma}$, the probability of false alarm for n^{th} channel under SINR value γ by evaluating the probability of the test statistic of the n^{th} channel greater than the threshold λ given the hypothesis $H0$. Steps 1 and 2 are repeated around 500 times each.

We group joint distribution of $P_d^{n,\gamma}$, $P_{fa}^{n,\gamma}$ corresponding to every γ as an interference class. Then, we apply the algorithm 1 in section IV to classify the interference class in each channel.

C. Selected results

We demonstrate the interference classification through experiments using the proposed testbed. We evaluated the performance metrics under each interference class for several thresholds. For every threshold, the moving average of 4000 iterations is performed to evaluate P_d and P_{fa}. Figure 4 shows the spectrum sensing performance under different interference scenarios using two different SDRs namely LimeSDR and USRP B205 mini. The interference classification is done offline using Python. LimeSDR has a good Receiver operating characteristics at in *Least* interference scenario while the *Medium* and *Worse* cases, USRP B205 mini has better operating characteristics compared to LimeSDR mini. Table II shows the KS_{OVR} and p-value for *Least*, *Medium*, and *Worst* cases for the considered channel. The KS_{OVR} for the *Least* and *Worse* have greater KS distance from other two classes. The p-value quantifies the level of confidence in this KS distance estimation. Figure 5 and Figure 6 shows the results of KS_{OVR} values for the test data using random forest and naive bayes classifier respectively. We can see that classification of *Least* interference from the other two classes are good. Whereas the classification of *Medium* and *Worst* classes from the other two classes is less useful.

VI. Interference Analysis using SALSAT Data

The fast Fourier transform (FFT) data is measured using a FPGA on board the Spectrum AnaLysis Satellite (SALSAT). This data is sent to the ground station for further analysis. The FFT message is sent with an id, frequency band, max hold

Table II
KS TEST RESULTS FOR INTERFERENCE CLASSIFICATION

Interference class	KS_{OvR}	p-value
Least(L)	0.75	0.8
Medium(M)	0.6	0.9
Worst(W)	0.05	1

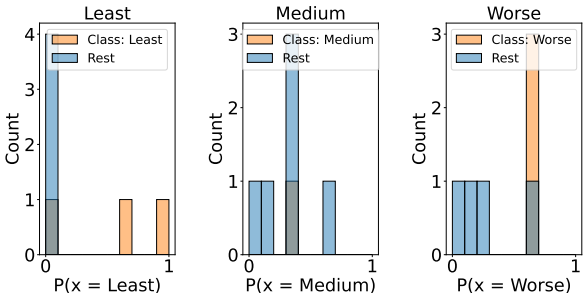

Figure 5. Kolmogrov-Smirnov one class over the rest (KS_{OVR}) for three interference classes using Random forest classifier.

duration, programmable gain settings of low noise amplifier, and programmable gain amplifier. Max hold duration will decide the number of time frames that are accumulated to increase the reliability of spectrum occupancy measurement. However, there is a trade-off between computational complexity and reliability. The higher the max hold setting, the higher is the computational complexity for an on-board SDR.

A. Kolmogrov-Smirnov test for backup channel prediction

The SALSAT data is preprocessed as each recording will have a different dynamic range of power spectral density (PSD)

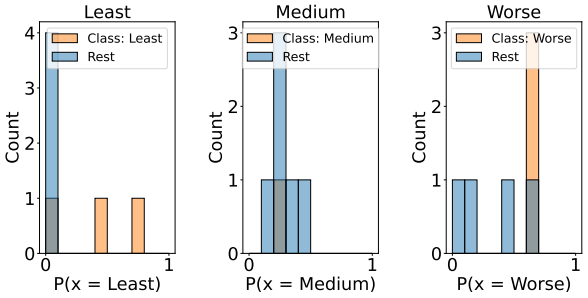

Figure 6. Kolmogrov-Smirnov one class over the rest (KS_{OVR}) for three interference classes using Naive Bayes classifier.

Table III
IMPACT OF PRE-PROCESSING METHOD OF DATA IN DETECTING AN UNCORRELATED DISTRIBUTION.

Pre-processing method	day	ks distance	p-value
minmax	1	0.46	1.06×10^{-10}
robust	1	0.1	0.20
minmax	2	0.37	9.35×10^{-6}
robust	2	0.18	0.15
minmax	3	0.67	1.36×10^{-9}
robust	3	0.37	0.02
minmax	4	0.99	6.22×10^{-84}
robust	4	0.3	1.4×10^{-6}

measured in dB. We considered two types of normalization techniques for pre-processing before KS test: (1) minmax normalization and (2) robust normalization. Robust normalization is particularly beneficial when data has many outliers. An FFT recording includes 4096 FFT bins which are equally divided into four channels ch1, ch2, ch3, and ch4 with 1024 bins each. The KS distance and p-value of the two channels aids in quantifying the similarity in their power spectral density distribution and is given by

$$D_{n,m} = \sup_x |F_{1,n}(x) - F_{2,m}(x)| \tag{7}$$

$D_{n,m}$ is a measure to quantify how likely the first sample of size n with empirical CDF $F_{1,n}(x)$ and second sample of size m with empirical CDF $F_{2,m}$ are similar. If samples from two channels have dissimilar distribution, then one channel can be used as a backup channel for the other channel. This method of comparison of distribution of channels aid in a backup channel prediction for the proposed cognitive radio.

B. Selected results

Figure 7 shows the cumulative distribution function (CDF) of PSD of ch1 and ch2 that was acquired over the a duration of 3 to 7 minutes of each satellite pass over four days. Table III shows that the p-value for robust normalization is greater than the minmax normalization. Hence, we have considered the robust normalization as the pre-processing step prior to train and test cycles of data. We can observe that the CDF of ch1 and ch2 for day1 and day2 has p-values greater than 0.05 for robust normalization case and shows that the distribution on these days are similar. While on day3 and day4, the p-values are smaller than 0.05 under both the normalization case and the distributions are different in these days. Hence, one of the channels can be used as a backup channel for the other on day3 and day4. This interference analysis from SALSAT data is a proof of concept that the backup channel can be predicted from the previous satellite pass data.

VII. CONCLUSION

In this paper, we studied the use of a cognitive radio-based interference analysis technique for use in satellite communication. In general, coexistence between satellite and terrestrial networks a very important aspect for next generation communication networks. We implemented an interference analysis algorithm for SDR for use in LEO satellites. Using both data from a cubesat mission (SALSAT) and experiments in a lab setup, we quantified the expected performance of the system. Our results show that the use for resilient critical infrastructure communication is possible. our insights will further be used in our project RACCOON, where the interference analysis can be performed by an on-board SDR to quickly adapt the communication parameters.

ACKNOWLEDGMENTS

The SALSAT mission and RACCOON payload development are funded by the Federal ministry for Economic Affairs and Climate Action (BMWK) through the German Bundestag

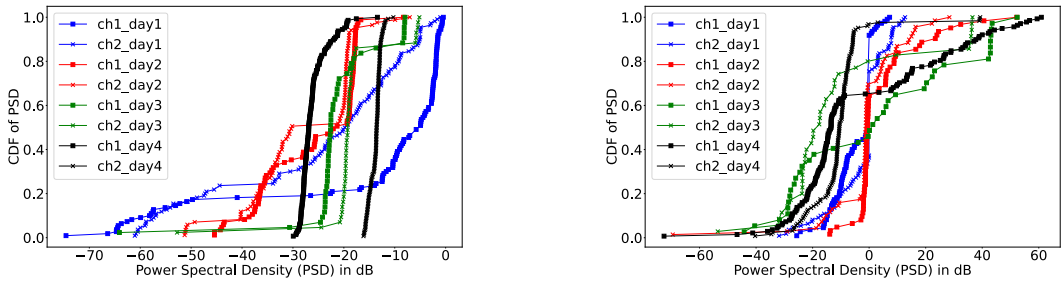

(a) PSD distribution with Minmax normalization on data

(b) PSD distribution with robust scaling on data

Figure 7. Cumulative distribution of PSD of the FFT frames acquired by SALSAT in UHF band

under grant no. 50 YB 1805 and 50 YB 2212. The SALSAT project team would like to express its gratitude to German Aerospace Center (DLR) for the continuous support and positive cooperation.

REFERENCES

[1] R. Radhakrishnan, W. W. Edmonson, F. Afghah, R. M. Rodriguez-Osorio, F. Pinto, and S. Burleigh, "Survey of Inter-Satellite Communication for Small Satellite Systems: Physical Layer to Network Layer View," *IEEE Communications Surveys & Tutorials*, vol. 18, no. 4, pp. 2442–2473, May 2016.

[2] F. Pinto, F. Afghah, R. Radhakrishnan, and W. W. Edmonson, "Software defined radio implementation of DS-CDMA in inter-satellite communications for small satellites," in *IEEE WiSEE 2015*, Orlando, FL, Dec. 2015, pp. 1–6.

[3] D. Giggenbach, A. Knopp, W. Mohr, M. T. Knopp, S. Schuster, and S. Hoppe, "NeSC - NewSpace Communications," VDE, VDE Positionspapier, Oct. 2023, pp. 1–32. [Online]. Available: https://www.vde.com/de/itg/publikationen/studien/vde-positionspapier-nesc-new-space-communications.

[4] G. Araniti, A. Iera, S. Pizzi, and F. Rinaldi, "Toward 6G Non-Terrestrial Networks," *IEEE Network*, vol. 36, no. 1, pp. 113–120, Jan. 2022.

[5] S. Narayana, R. V. Prasad, V. S. Rao, L. Mottola, and T. Venkata Prabhakar, "A Hummingbird in Space: An energy-efficient GPS receiver for small satellites," *GetMobile: Mobile Computing and Communications*, vol. 25, no. 1, pp. 24–29, Jun. 2021.

[6] J. Großhans, M. Buscher, H. Q. Vu, A. Balke, A. Maaß, and A. Lohse, "SALSA-A novel Spectrum Analyzer board for LEO Satellite Allocations based on SDR technology," in *AIAA SPACE and Astronautics Forum and Exposition*, Virtual Conference, Sep. 2018, p. 5283.

[7] F. Dressler, "Physical Layer Resilience through Deep Learning in Software Radios: Technical Perspective," *Communications of the ACM*, vol. 65, no. 9, pp. 82–82, Sep. 2022.

[8] J. Mitola, A. Attar, H. Zhang, O. Holland, H. Harada, and H. Aghvami, "Achievements and the Road Ahead: The First Decade of Cognitive Radio," *IEEE Transactions on Vehicular Technology*, vol. 59, no. 4, pp. 1574–1577, May 2010.

[9] A. Zubow, M. Döring, M. Chwalisz, and A. Wolisz, "A SDN approach to spectrum brokerage in infrastructure-based Cognitive Radio networks," in *IEEE DySPAN 2015*, Stockholm, Sweden: IEEE, Sep. 2015.

[10] F. Rinaldi, H.-L. Maattanen, J. Torsner, S. Pizzi, S. Andreev, A. Iera, Y. Koucheryavy, and G. Araniti, "Non-Terrestrial Networks in 5G & Beyond: A Survey," *IEEE Access*, vol. 8, pp. 165 178–165 200, 2020.

[11] H.-W. Lee, A. Medles, V. Jie, D. Lin, X. Zhu, I.-K. Fu, and H.-Y. Wei, "Reverse Spectrum Allocation for Spectrum Sharing between TN and NTN," in *IEEE CSCN 2021*, Thessaloníki, Greece: IEEE, Dec. 2021.

[12] L. G. Barros Guedes and D. A. Guimarães, "Performance of Detectors for Cooperative Spectrum Sensing Under Laplacian Noise," *Journal of Communication and Information Systems*, vol. 39, no. 1, pp. 1–12, Jan. 2024.

[13] G. Quintana-Diaz, T. Ekman, J. M. Lago Agra, D. Hurtado de Mendoza, F. Aguado Agelet, and A. González Muíño, "In-Orbit Measurements and Analysis of Radio Interference in the UHF Amateur Radio Band from the LUME-1 Satellite," *Remote Sensing*, vol. 13, no. 16, p. 3252, Aug. 2021.

[14] J. Großhans, P. Wüstenberg, A. Balke, T. Vanichangkul, M. Pust, E. Stoll, and S. Voigt, "SALSAT: First mission results of the global RF spectrum analysis in the VHF, UHF and space research bands measured by the Spectrum Analysis SATellite," in *International IAC 2022*, Paris, France, Sep. 2022.

[15] J. Großhans, P. Wüstenberg, H. Q. Vu, A. Balke, F. Baumann, D. Noack, M. Pust, H. Adirim, F. Lang, T. Funke, T. Vanichangkul, and E. Stoll, "Small Satellites for Cyber Security Applications at the TU Berlin - the RACCOON and CyBEEsat missions," in *International IAC 2022*, Paris, France, Sep. 2022.

[16] K. Pelechrinis, P. Krishnamurthy, M. Weiss, and T. Znati, "Cognitive radio networks: realistic or not?" *ACM SIGCOMM Computer Communication Review*, vol. 43, no. 2, pp. 44–51, Apr. 2013.

[17] A. Jain, B. Amrutur, and S. Vinod, "Soft real time implementation of a Cognitive Radio testbed for frequency hopping primary satisfying QoS requirements," in *National NCC 2014*, Kanpur, India: IEEE, Feb. 2014, pp. 1–6.

[18] R. Prasanna and B. Amrutur, "Cognitive radio implementation for a frequency hopping primary signal," in *National NCC 2013*, New Delhi, India: IEEE, Feb. 2013.

[19] L. Franck, T. Benaddi, and L. B. Cardoso da Silva, "Cognitive Radio Overlay Paradigm Towards Satellite Communications," in *IEEE BlackSeaCom 2018*, Batumi, Georgia: IEEE, Jun. 2018, pp. 1–5.

[20] T. Yucek and H. Arslan, "A survey of spectrum sensing algorithms for cognitive radio applications," *IEEE Communications Surveys & Tutorials*, vol. 11, no. 1, pp. 116–130, Mar. 2009.

[21] M. Liu, N. Zhao, J. Li, and V. C. M. Leung, "Spectrum sensing based on maximum generalized correntropy under symmetric alpha stable noise," *IEEE Transactions on Vehicular Technology*, vol. 68, no. 10, pp. 10 262–10 266, May 2019.

[22] E. Axell, G. Leus, H. V. Poor, and E. G. Larsson, "Spectrum Sensing for Cognitive Radio : State-of-the-Art and Recent Advances," *IEEE Signal Processing Magazine*, vol. 29, no. 6, pp. 101–116, Nov. 2012.

[23] S. Gurugopinath, C. R. Murthy, and C. S. Seelamantula, "Zero-crossings based spectrum sensing under noise uncertainties," in *National NCC 2014*, Kanpur, India: IEEE, Feb. 2014, pp. 1–6.

[24] S. Aghabeiki, C. Hallet, N. E.-R. Noutehou, N. Rassem, I. Adjali, and M. Ben Mabrouk, "Machine-learning-based spectrum sensing enhancement for software-defined radio applications," in *IEEE CCAAW 2021*, Cleveland, OH: IEEE, Jun. 2021.

[25] C.-S. Choi, "Modeling and Analysis of Downlink Communications in a Heterogeneous LEO Satellite Network," *IEEE Transactions on Wireless Communications*, vol. 23, no. 8, pp. 8588–8602, Aug. 2024.

[26] C.-S. Choi and F. Baccelli, "Cox Point Processes for Multi Altitude LEO Satellite Networks," *IEEE Transactions on Vehicular Technology*, vol. 10, pp. 1–6, Jun. 2024.

[27] P. J. L. Adeodato and S. B. Melo, "On the equivalence between Kolmogorov-Smirnov and ROC curve metrics for binary classification," arXiv, cs.AI 1606.00496, Jun. 2016.